The estimation of intracranial pressure using blood pressure signals.

Author: Cees Jan DRONKERS

Supervisors: Prof. Dr. Anton STOORVOGEL
University of Twente
Mw. Dr. Astrid HOEDEMAEKERS
UMC St Radboud, Nijmegen

UNIVERSITY OF TWENTE

October 7, 2011

Abstract

Reliable estimation of intracranial pressure can decrease the need for invasive ways to measure it directly. A study was done on the usability of blood pressure signals(primary arterial pressure and jugular venous pressure and also central venous pressure) in intracranial pressure estimation. Different ideas are applied to study interconnections in the data, using mathematical techniques like frequency analysis and AR-modelling. Also, an overview is given of recent attempts to construct a model of the intracranial pressure system.

The main conclusion is that intracranial pressure estimation using only blood pressure signals is not possible. Some minor positive results surfaced when looking at the influence of intracranial pressure on the structure of the jugular venous pressure signal.

Preface

For the last nine month, I have been doing research at the University of Twente and in the Radboud hospital. My goal was to look for ways to estimate intracranial pressure using other available measurements. It have been interesting months. I got fascinated by the complex dynamics of the human body and I learned a lot by trying to understand it. The fact that my research resulted in a mainly negative answer sometimes gave some motivational difficulties, but this also thought me a lot about research. It have been interesting times.

I would like to thank prof. Stoorvogel for his supervision and critical view. And I would also like to thank drs. Hoedemaekers for giving me the opportunity to do this project and for helping me as a student without any medical background to get some understanding about the human body. Finally, I would like to thank my wife, family and friends for their support and the sometimes necessary cheer-ups.

This report is the result of my research. I hope, it will give a clear view on both the positive and negative results of this study. Enjoy reading!

Cees Jan Dronkers, October 2011

Contents

List of Acronyms

ICP	Intracranial pressure
ABP	Arterial bloodpressure
JVP	Jugular venous pressure
CVP	Central venous pressure
CPP	Cerebral Perfusion Pressure
CBF	Cerebral bloodflow
CSF	Cerebrospinal fluid
AR-model	Autoregressive model
ARX-model	Autoregressive model with external input

1 Introduction

1.1 Clinical context

The subject of this thesis is the estimation of intracranial pressure(ICP)[1]. After acute brain trauma, this pressure plays an important role in critical care(the reason for this will be given in subsection 1.2.2). Because of this, ICP is often measured.

The most common way to measure ICP is visualized in figure 1. A hole is drilled in the skull, a catheter is inserted through this hole and the brain matter into the lateral ventricle[2]. Through this catheter, the pressure in the lateral ventricle can be measured and this pressure is assumed to represent ICP in general cases. This procedure is rather invasive and entails a large infection risk, certainly, when the measurement continues for more than five days[Rebuck et al., 2000]. Because of this, less risky ways to measure or estimate ICP would be beneficial to brain trauma patients. This report describes a search for ways to estimate ICP.

1.2 Biomedical context

First, an outline of intracranial anatomy will be given. After this, the importance of intracranial pressure in neurological intensive care will be explained and the issue of pressure homogeneity will be addressed. Finally, a short overview will be given of relevant quantities for intracranial pressure estimation.

1.2.1 Intracranial anatomy

An schematic illustration of this outline is given in figure 2. A large part of the intracranial space is occupied by fluids, namely blood and cerebrospinal fluid(CSF). The blood supplies the brain with oxygen and other required substances and it removes carbon dioxide and cellular waste products from the brain. From all these functions, oxygen supply is the most vital one, because lack of oxygen can lead to brain damage in a matter of minutes. Blood is supplied by the cerebral arteries and drained by the jugular veins.

The main function of CSF is protection of the brain matter. The brain matter is floating in the CSF and this causes it to be less sensitive to sudden movement of the head. CSF is generated mainly in the choroid plexus[3] and drained in the dural venous sinuses[4], back into the blood stream. It's dynamic nature gives it the ability to adapt CSF volume.

When the amount of liquid(blood and CSF) inside the cranium rises, the ICP will rise. The cranium itself is almost totally rigid, but the brain-matter is rather elastic, causing the compartment of intracranial liquids(space in the brain occupied by blood en CSF) to be compliant. The relationship between pressure and volume(blood and CSF) in the brain was already described by Marmarou

---

[1]Intracranial means within(intra) the cranium. The cranium is the top top part of the skull, containing the brain.

[2]A cavity in the center of the brain which holds brain fluid.

[3]Tissue in the brain which transports fluid from the bloodstream into cavities which are called ventricles.

[4]The dural venous sinuses are small veins, close to the skull. They drain blood from the brain into the internal jugular vein, which in turn brings it back to the heart.
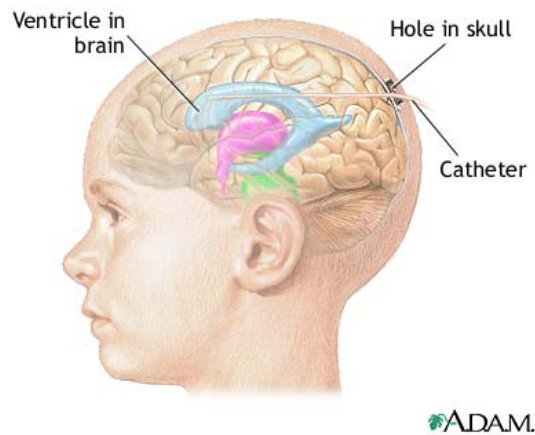
Figure 1: In most cases, ICP is measured through a catheter inserted into the lateral ventricle. Image from [Dugdale and Hoch, 2011].

in 1975[Marmarou et al., 1975].

1.2.2 Importance of ICP

Brain trauma can result in internal hemorrhaging(bleeding), causing the amount of liquid in the brain to increase. Due to the rigidness of the skull, this will give an increase in intracranial pressure. So after acute brain injury, patients have an increased risk of elevated ICP. The blood supply to the brain is governed by the difference between the arterial pressure and the ICP. This difference is called the Cerebral Perfusion Pressure(CPP). To ensure adequate oxygen supply to the brain, the blood supply should stay above a certain level and therefore, the CPP should be sustained above a certain level. A process called cerebral autoregulation will keep the cerebral blood flow(CBF) constant by adjusting the vascular resistance[5]. This is done inducing vasodilation or vasoconstriction and will respectively lower or heighten the vascular resistance. Of course, this process will only work within a certain range of ICP, above which the blood supply to the brain will decrease. Because of this, increased ICP is associated with high mortality and high risk of neurological damage. This is why ICP should be monitored if there is a significant chance that it will increase.

1.2.3 Pressure homogeneity

By using one pressure value to represent the ICP, it is implicitly assumed to be homogeneous throughout the skull. Of course the ICP is not totally homogeneous, but in most cases the inhomogeneity of the ICP is not significant within a clinical context. Therefore, ICP will be assumed to be homogeneous within

---

[5]Resistance of the blood vessels
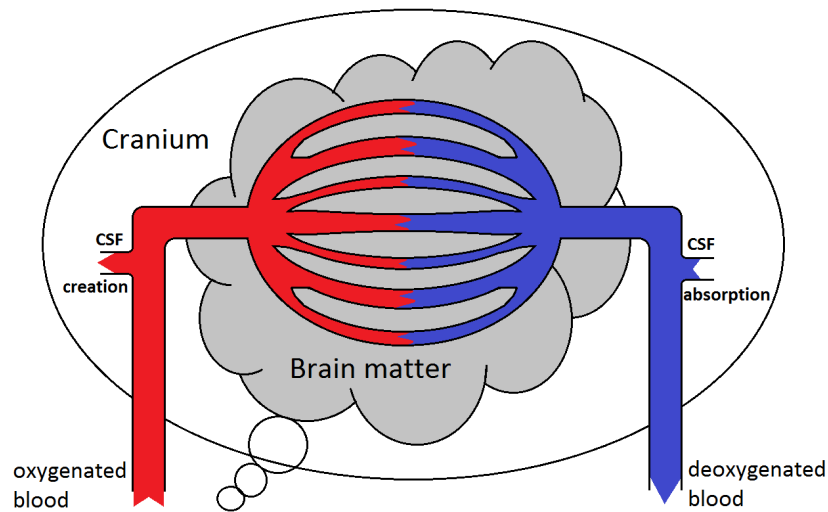
Figure 2: Schematic figure of brain anatomy.

the scope of this report[6].

1.2.4 Measurement options

Relevant quantities available for measurements can be divided into three categories; pressures, flows and other quantities.

Pressure quantities are relatively easy to measure. An open connection between the measurement point and a pressure transducer[7] can be created using a catheter. This method is used to continuously measure arterial blood pressure(ABP) of all ICU-patients. This signal is measured in the arm, but is assumed to be approximately equal to arterial pressure in the common carotid artery[8] except for a time shift.

The jugular venous pressure(JVP)[9] is not measured by default, but can be obtained by inserting a catheter into the inner jugular vein. Because of the influence of heartbeat dynamics on the JVP, central venous pressure(CVP)[10] also is an interesting quantity. In some cases, this pressure can be measured using an existing catheter, which is normally used to take blood samples.

The ICP is already measured and therefore it can also be easily obtained for research purposes. The measurement method in the Radboud hospital is slightly different from the one described in subsection 1.1. The pressure is not measured in the ventricles, but in the brain matter, using a similar technique.

---

[6]In special cases, a local increase in pressure can cause problems while the pressure in the lateral ventricle remains unchanged. In this case, local pressure measurements and/or MRI-scans are used for monitoring.

[7]A device which generates a signal as a function of the imposed pressure.

[8]The artery which provides oxygenated blood to the head and the neck.

[9]Pressure in the veins which drain deoxygenated blood from the brain.

[10]The blood pressure where the veins enter the heart.

Flow quantities are the most insightful quantities to work with. When we measure in- and outflow, it should be relatively easy to detect volume changes(and therefore pressure changes) in the brain. However, it is difficult to measure them and even if it can be measured, accuracy is an issue. At the moment, the only operational way to measure arterial blood flow is using flow velocity measurements, because measuring velocity is easier than measuring flow. Velocity can be measured using transcranial Doppler(TCD)[Aaslid et al., 1982]. It is non-invasive, but rather operator dependent and mainly useful to detect flow differences. To estimate blood flow, the artery diameter has to be measured or estimated, which is also very difficult to do in an accurate way. Because of the complexity of flow measurement, no flow measurements were done in the context of this research.

Apart from blood flow and pressure, other quantities can also be interesting. Brain matter oxygenation levels can be measured using non-invasive infrared measurements(for examples using the INVOS system[INVOS, 2011]). One also could measure carbon dioxide concentrations in the jugular vein to study brain oxygenation.[Kuwabara et al., 1992]. These quantities have not been included in this research, but could prove to be interesting.

1.3 Research goal and methods

We have seen that knowing the ICP is crucial for accurate diagnosis and monitoring after acute brain injury. Measuring it directly is an invasive procedure, which is not preferable when the patients health is critical. Therefore estimating ICP using only non-invasively measured signals would give physicians a powerful tool for diagnoses without increasing the risk for the patient.

Available signals which are measured non-invasively, are arterial blood pressure and jugular venous pressure. Our question is the following:

1. Is it possible to extract information about intracranial pressure from cerebral pressure signals(arterial and venous pressure)?

2. How can we extract this information?

To find answers to these questions, several approaches will be addressed. In section 2 correlation techniques will be used to study the connection between ICP and JVP. In section 3, the influence of CVP on JVP is studied using frequency analysis. In section 4 the connection between ICP and JVP waveform is examined and in section 5, the possibilities and limitations of models for ICP estimation are explored. This results in an investigation on the use of estimated model parameters in ICP estimation.

1.4 Data acquisition

All data was acquired on the neuro-ICU in the Radboud hospital in Nijmegen. The ICP and ABP are already measured. For JVP measurement, a catheter was inserted into the jugular veins and connected to a pressure transducer. For

CVP measurement, an existing catheter was connected to a pressure transducer (this was only done for one patient). All signals were acquired using an AD-converter which was connected to a laptop. Labview Signal Express software was used to record the signals at a sample frequency of 200Hz.

In the report, 39 hours and 51 minutes of measurement data was used. The data was acquired from three different patients on nine different days. During the last measurement sessions CVP was recorded alongside APB, ICP and JVP. From the datasets, 76 10-minute samples were extracted for analysis. The samples were selected manually, based on stationarity of the ICP signal. In appendix A, an overview is given of the datasets and 10-minute samples.

Normally ICP varies between 7.5 and 15 mmHg. It is considered elevated if it is above 20 mmHg. The mean ICP values in the samples of patient $1(n = 19)$ range from average to high ICP. Samples from patient $2(n = 8)$ only give average ICP measurements(with one exception of an elevated reading). Mean ICP values for patient $3(n = 49)$ range from very low to high.

For each sample the Pressure Reactivity index(PRx) was calculated. This is the cross-correlation[11] between ABP and ICP and it is assumed to give some insight in autoregulation functionality[Smielewski et al., 1997]. A negative PRx indicates functional autoregulation, while a positive PRx indicates impaired autoregulation. The cross-correlation was calculated from a smoothened and downsampled version of the signal. Note that the dataset is less extensive than the datasets which are used in research concerning PRx and therefore, accuracy might be a problem. The values indicate working autoregulation for patients 1 and 2 and impaired autoregulation for patient 3.

---

[11]Cross-correlation is a measure of similarity of two signals. Positive cross-correlation indicates that the signals tend to increase and decrease simultaneously. Negative cross-correlation indicates that the signals behave opposite to each other (if one increase, the other one decreases).

2 Connection between ICP and JVP

2.1 The idea

When analyzing interconnection between different signals, the cross-correlation between the signals plays an important role. The maximum of the cross-correlation(maximized over time lag) between the blood pressure signals and the intracranial pressure signal is rather high(0.69 ± 0.15 for venous pressure and 0.77 ± 0.06 for arterial pressure). This appears to give opportunities for ICP estimation. But careful examination is required to draw conclusions based on (cross-)correlations.

If two signals from disconnected systems have similar structure(for example a trend or periodical behavior), their cross-correlation will be very high. Based on this fact, one could wrongly assume a connection between the systems. In our case, both signals have a lot of structure and periodical behavior. This could be the source of a lot of correlation.

To study the real interconnection between signals, they need to be corrected for this. This can be done by looking for structure in the signal and subtracting it from the signal. The remaining part is called noise. Systems which are really interconnected should also show correlation between the noise signals, because a disturbance in one of the systems should be observable in the other system (an explanation of the mathematics behind this idea can be found in subsection 2.2)

2.2 The math

To correct the correlation for structure in the signals, the signals are modeled by an autoregressive(AR)-model with an additive stochastic component:

$$p(t) = \sum_{i=1}^{k} \alpha_i p(t - i) + w(t) \tag{1}$$

$p(t)$ is the pressure at time t, $w(t)$ is the stochastic component at time t and α_i are the model parameters. Using a least-squares optimization, the model parameters can be estimated. From the original signal and the model parameters, $w(t)$ can be calculated for all signals. So now we have $w_{jvp}(t)$, $w_{abp}(t)$ and $w_{icp}(t)$. Interdependency between ICP and JVP should be observable in correlation between $w_{jvp}(t)$ and $w_{icp}(t)$.

The stochastic components were calculated for different model orders(2, 4 and 6). The resulting correlations are shown in table 1. This shows that the correlation between the signals originates almost entirely from a mutual external 'deterministic' origin.

Because correlation only takes linear relationships into account, the squares of the signals was also used to calculate cross correlations(between squared signals and between one signal and the square of the other signal). This resulted

	2	4	6
ABP	0.046 ± 0.063	0.027 ± 0.066	0.017 ± 0.054
JVP	0.056 ± 0.033	0.023 ± 0.027	0.024 ± 0.024

Table 1: Mean of maximum cross correlation values between the stochastic parts of ICP and the blood pressure signals for several model orders. The mean was calculated over a set of 76 samples from three different patients.

in similar lower correlation coefficients(< 0.09) with the same inter-sample consistency, indicating that a non-linear approach will not help.

2.3 Results

In table 1, maximum cross-correlation-values between ICP and the arterial and venous blood pressure noise signals are shown. Maximum cross-correlation was calculated for 76 10-minute samples. The model orders are the degree of complexity of the model which was used to model the structure in the signals.

In chapter 3.4, it is shown that the connection between ICP and JVP is less dominated by the heart at low frequencies. Because of this, and because we are mostly interested in long range ICP behavior, it is interesting to look for correlation at very low frequency. In order to do this, we look at the mean pressure levels of the 10-minute samples. Figure 3 shows scatter plots of these pressure levels. Within the same day, the samples show a great consistency in arterial and venous pressure, while intracranial pressure varies a lot. No significant correlation can be found on the whole set or in the sets of separate days. Any significant correlation in patient sets is due to clustering of values.

After correction for structure, the cross-correlation coefficients do not significantly differ from zero and therefore, we can conclude that there is no clear connection between the blood pressure signals and the ICP signal. Correlation analysis in the very low frequency range also shows no clear correlation between the signals.
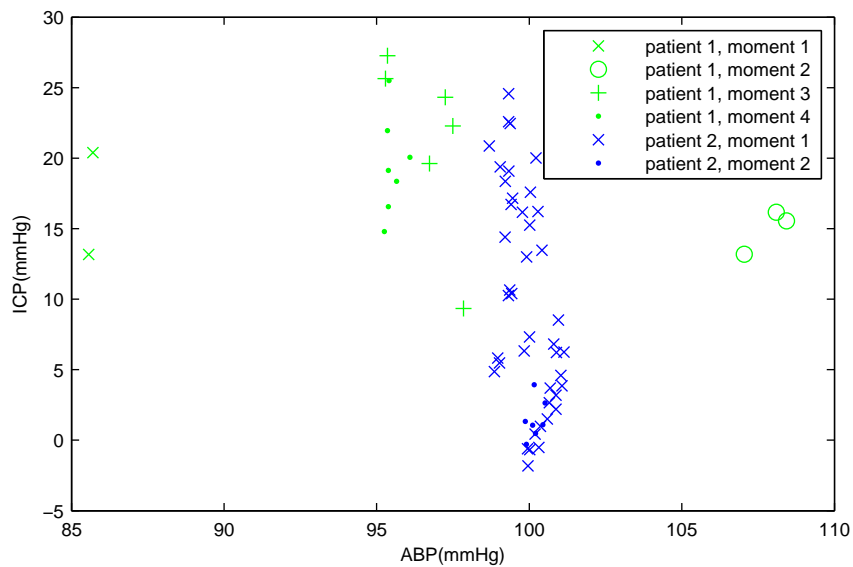
(a) ABP correlations
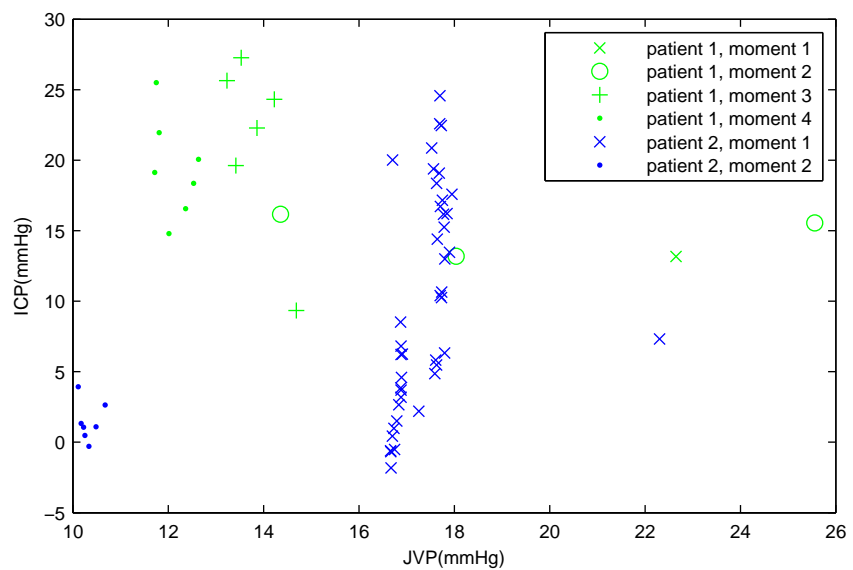
(b) JVP correlations

Figure 3: Scatter plot between blood pressure means and the ICP mean. The mean is calculated over 10-minute samples

3 Connection between JVP and CVP

3.1 The idea

Because of the blood flow direction, the JVP is the pressure signal which is the most likely to contain information about ICP. ABP is mainly influenced by cardiac and pulmonary activity and vascular bed resistance, while JVP should be influenced by blood flow from the brain. However, it is generally believed that pressure waves in the venous system mainly travel upstream[12]. To study if this is indeed true, we first look at the time-difference in heartbeat waveforms between the two signals. Figure 4 shows the CVP signal and the JVP signal. The mean time difference from a CVP peak to a JVP peak for all sets is 0.32 ± 0.07, giving a pressure wave velocity of $0.78\ m \cdot s^{-1}$. The mean time difference between a JVP peak and the next CVP peak, it is 0.55 ± 0.13, which would require a pressure wave velocity of $0.45\ m \cdot s^{-1}$. Upstream blood pressure wave velocities have been reported to be approximately $1\ m \cdot s^{-1}$[Hellevik et al., 1999] while downstream velocities are higher(arterial pressure waves normally have a velocity of around 8 $m \cdot s^{-1}$[Koivistoinen et al., 2007]). From this, we can conclude that the heartbeat pressure wave is going upstream.

Frequency analysis tools will be used to study periodical behavior in the signals.
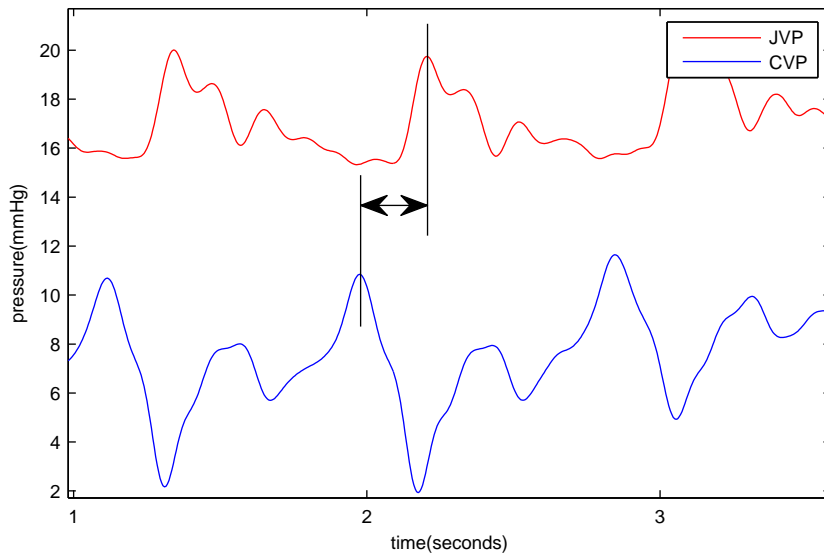

Figure 4: Plotting the JVP and CVP together clearly shows that the CVP peaks earlier than the JVP.

3.2 Frequency spectrum analysis

The signals which are studied are highly periodical. There is a very dominant heartbeat and the respiratory cycle can also clearly be recognized in the signal.

---

[12]The JVP has actually been used in clinical context to estimate CVP.

A mathematical technique, called the Fourier transform, can be used to study periodical behavior. Applying the Fourier transform to a signal gives the intensity of the signal in a range of frequencies.

In figure 5, an example of a Fourier spectrum is shown. The high peak at 1.25
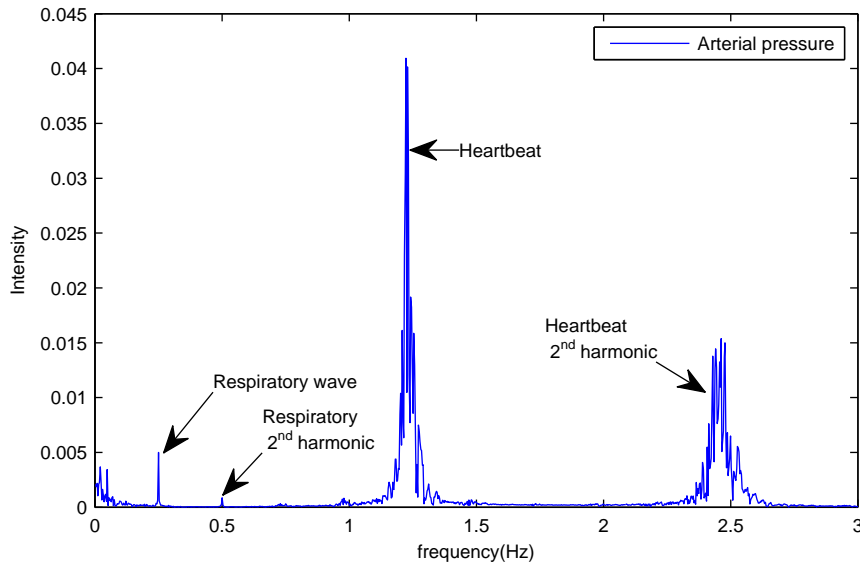
Figure 5: An example of a Fourier-spectrum of an arterial bloodpressure signal

Hz is representing the heartbeat(1.25 Hz or = 80 beats per minute). It is clearly the most dominant peak in the spectrum. The peak at 2.5 Hz is also caused by the heartbeat. It is called the second harmonic and it's frequency is exactly twice as high as the first harmonic(the peak at 1.25 Hz). This phenomenon is well known in mathematics and physics. It is caused by the fact that the heartbeat waveform is not a sine[13]. The heartbeat waveform also has higher harmonics(for example at three times the frequency), but these are not in range of this figure.

The respiratory function is also visible in the Fourier spectrum. It is a peak at 0.25 Hz(respiratory rate of 15 breaths per minute) with a second harmonic at 0.50 Hz. This peak is very narrow because the breathing frequency is very constant due to mechanical ventilation. Compared to this, we see that the heartbeat is more variable(the peak is wider).

Finally, we see a rise of the spectrum when going to the very low frequencies. This represents very slow changes in the signal. In this part of the spectrum, a small peak is present in most of the spectra(this is not clear in figure 5, but it is in figure 6(a) at approximately 0.05 Hz). This periodic behavior appears to be caused by the compression system which stimulates the venous blood flow in the legs(it is documented to operate between 0.02 Hz and 0.05 Hz).

Next to visual examination of the spectra, it would be convenient to have a

---

[13]A well known example of higher harmonics are the harmonics of sound. When different musical instruments play the same note, they sound different. This is due to a different waveform of the sound wave(in the time-domain). In the frequency domain, the difference is represented in a different relative magnitude of the harmonics.

measure for correspondence between between two frequency spectra. Finding such a measure is not self-evident. Within the context of this report a measure was used which is based on correspondence of up and downward movement of the spectrum:

$$\text{Correspondence} = \frac{\text{\# Of matching up or downward movements}}{\text{\# Of movements}} \quad (2)$$

This measure is explained in more detail in 3.3.

3.3 The math

A good measure for correspondence between Fourier spectra is hard to find. The transfer function between strongly connected systems will almost never be 1 or even constant, so matching the spectra themselves(for example in an MSE-way) would be tricky. Because of this, a measure was developed which is based on a match of derivative sign. Let F_ω and G_ω with $\omega \in \{\omega_k \mid 1 \leq k \leq n \wedge \omega_1 < \omega_2 < \ldots < \omega_n\}$ be two frequency spectra, then

$$M(F, G) = \frac{|\operatorname{sgn}(\bigtriangledown G) - \operatorname{sgn}(\bigtriangledown F)|}{n - 1} \quad (3)$$

The choice for this measure is based on the assumption that the transfer function between the signals is smooth. In this case, local differences should be dominant over the transfer function derivative. Because the measure was only used to gain some initial insight, it was not fully tested or verified.

3.4 Results

ICP, JVP and CVP measurements have been acquired from one patient on two different days. 49 10-minute samples were isolated. The heartbeat frequency peak of the ICP, JVP and the CVP signal(a representative example can be found in figure 6(a), in this figures, the spectra have been normalized to make observations easier) do almost totally match. This indicates a very clear link between the signals. Because the system, influencing the CVP is big (the whole venous system and the heart), we can assume that this match is caused by a dominant influence of heartbeat dynamics on the vein pressure and on ICP.

This behavior is visible in the whole frequency range except for very low frequency(figure 6(b)). In this range(< 0.12 Hz), the ICP and JVP signal still behave approximately the same, but the CVP behaves differently.

Using the measure described in subsection 3.3, the similarity between the spectra at different frequencies was calculated. For high frequency, the range 1.1-1.4 Hz was selected, because of the heartbeat dynamics in this range. For low frequency, the range 0.02-0.12 Hz was selected because this part of the spectrum contains slow changes in the signal. In figure 7, a boxplot is shown of the similarity between the Fourier spectra at different frequency ranges for the 49 samples. At high frequency, similarity between all the signals is high. At low frequency, it shows a significantly lower similarity between CVP and ICP. In this frequency range, correspondence between JVP and ICP cannot totally be explained by dominating heart dynamics influencing both signals. Therefore,

it may be possible that JVP contains information about ICP in this frequency range.


(a) Low frequency
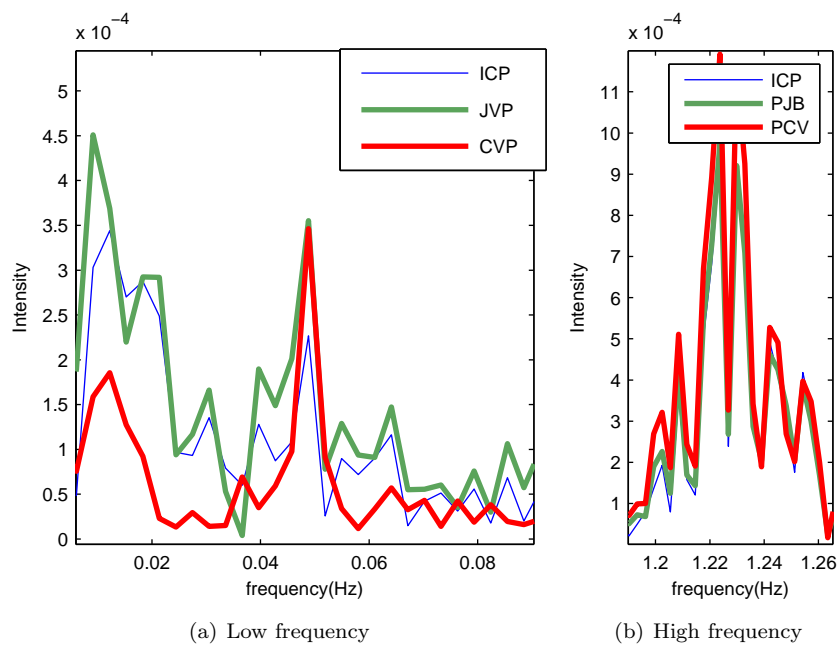
(b) High frequency

Figure 6: Comparison between frequency spectra of ICP, JVP and CVP of a representative 10-minute sample. The intensities are normalized.
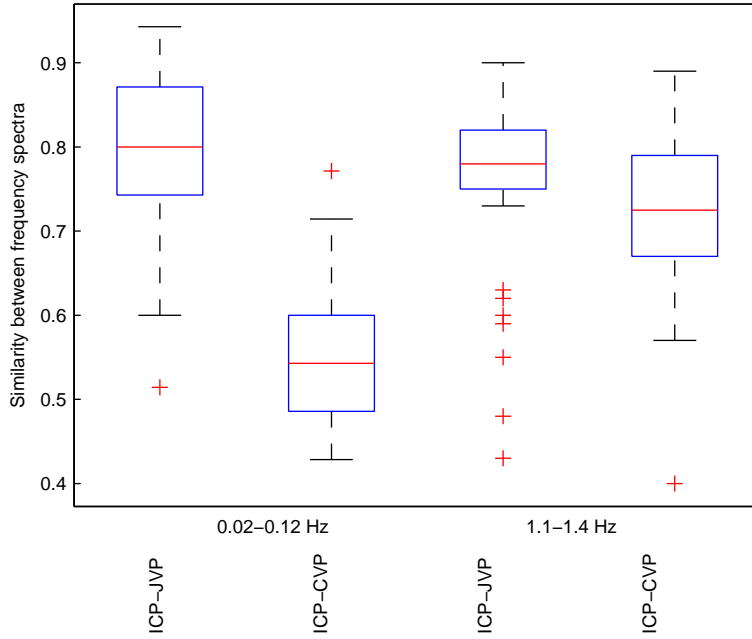
Figure 7: Calculated match between JVP and ICP/CVP for low and high frequency.

4 JVP Waveform analysis

4.1 The idea

It is thought that ICP influences the waveform of the JVP. Frequency analysis can also be used to get information about waveform shapes of the two dominant waves(heartbeat and breathing). Figure 8 illustrates how a difference in waveform is reflected in the Fourier-spectrum of a signal. To the left, three time signals are shown with the same period(2 seconds) and the same power[14]. Its frequency spectrumis shown to the right. In this figure, the frequency spectra of the block-wave and the sawtooth-wave are slightly shifted to be able to distinguish between the different signals. They all have peaks at multiples of 1 Hz. The sine(blue) only has a peak at 1 Hz(it's frequency) and no higher harmonics[15]. On the other side, the block wave and the sawtooth wave have clearly distinguishable peaks at multiples of 1 Hz in the frequency spectrum. The difference between the signals is inner-wave symmetry of the signal. The block wave is half-wave symmetric[16], while the sawtooth-wave is not[17].

This example shows that the magnitude of the higher harmonics gives information about the shape of the signal. This can be used for analysis of the JVP signal, but for this, some practical remarks have to be made. For accuracy reasons, only the first few harmonics can be used(the peaks get smaller at higher

---

[14]power is a mathematical term, indicating the amount of energy in a signal per time unit.
[15]The concept of harmonics was explained in subsection 3.2
[16]Meaning the second half is equal to the first half, mirrored in the time axis.
[17]A mathematical explanation of this behavior can be found in subsection 3.3

frequency). Because inner-wave symmetric changes will affect the odd harmonics, while asymmetric changes will influence even harmonics, it is advisable to study an odd and an even harmonic. Because of these reasons, the second and the third peak will be studied. Peak magnitude can be measured by calculating the area under the peak. In order to eliminate influence from a difference in signal energy, the peak magnitude should be normalized. This is done by dividing it by the magnitude of the first harmonic(in the example the peak at 1 Hz). So

$$2^e \text{ harmonic normalized magnitude} = \frac{2^e \text{ harmonic magnitude}}{1^e \text{ harmonic magnitude}} \tag{4}$$

The same holds for the third harmonic normalized magnitude. If there is a relation between ICP levels and JVP waveform, it could present itself in a relation between ICP levels and second and/or third harmonic normalized magnitudes of the JVP signal. An absence of this relation on the other hand, would indicate that ICP levels do not influence JVP signal shape.

(a) Time-domain

(b) Frequency-domain, the spectra if the block- and sawtooth wave are slightly shifted to be able to distinguish between the signals.
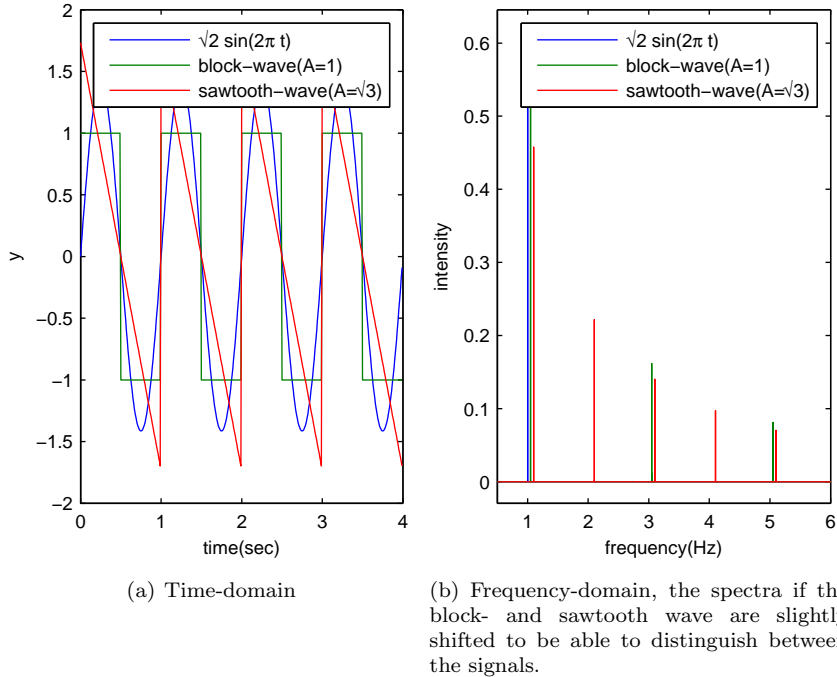
Figure 8: Fourier-transform of several basic time-signals.

4.2 The math

Inner-wave symmetry is a property of a wave in a signal. Mathematically, it means that

$$f(t) = -f(t + \frac{T}{2}) \tag{5}$$

where f is the wave part of the signal and T is its frequency. Possible higher harmonic components of a wave with fundamental frequency T will either be

14

inner-wave symmetric at frequency T or not inner-wave symmetric at frequency T:

$$- f(t + \frac{k}{2}T) = \begin{cases} -(f(t)) & k \text{ even} \\ (f(t)) & k \text{ odd} \end{cases} \tag{6}$$

This explains why the even harmonic components do not contribute to an inner-wave symmetric wave and illustrates the value of analyzing more than one higher harmonic component of the wave.

4.3   Results

In section B.1, the calculated correlation values can be found. While respiratory waveform harmonics do not show any significant correlation, heartbeat waveform harmonic intensities do highly correlate with ICP. The positive correlation is consistent for all patients when one outlier is omitted from the patient 2 set[18]. And except for the second harmonic intensity from patient 2, all correlations are highly significant.
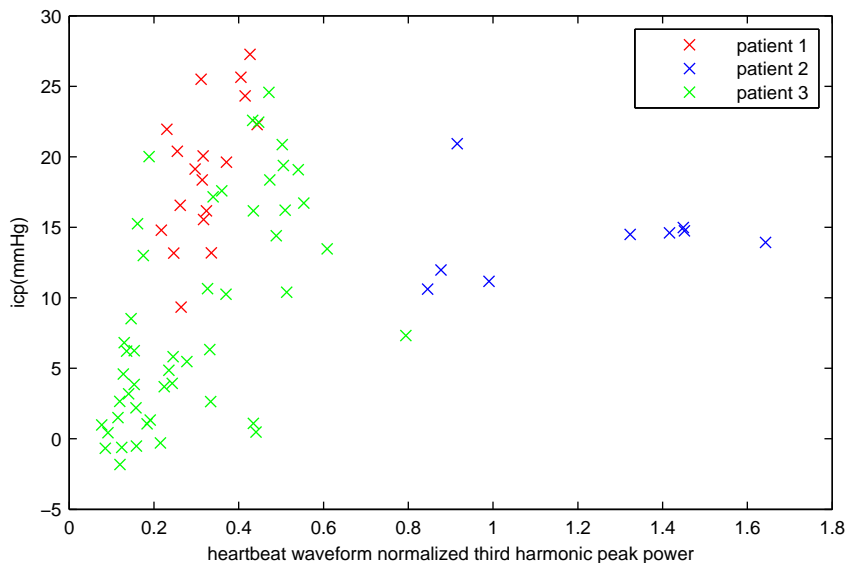
Figure 9: Scatter plot of normalized third harmonic intensity(heartbeat waveform) vs. ICP.

The question can be posed if the two parameters carry the same information. If this is the case, one of the two could be ommited without losing information. To answer this question, we take a look at the relationship between the parameters.

Correlation between the second and the third harmonic intensity for the heartbeat waveform is 0.79(0.92, 0.70 and 0.88 for individual patients). The partial

---

[18]Without outlier, patient 2 had correlations of $0.84(p = 0.009)$, $0.53(p = 0.172)$, $0.54(p = 0.163)$, $0.89(p = 0.003)$ respectively for the respiratory waveform 2nd and 3rd harmonic and the heartbeat waveform 2nd and 3rd harmonic.

correlations with ICP, [19] are not very consistent, but certainly not zero(0.44, -0.70 and -0.05 for the second harmonic intensity and -0.42, 0.59 and 0.38 for the third harmonic intensity for individual patients). So there could be a little extra information in the combination of the two, but evidence is not overwhelming or consistent[20].

Figure 9 shows the connection between third harmonic relative intensity and ICP. For each of the patients, the correlation is very clear. However, this does not result in clear global correlation. The relation between higher harmonic intensities and ICP values seems to be very patient-specific.

5   White-box model approach

The first part of this section will be an explanation of the concept of a white-box model and the possible use of this concept within the scope of this research will be explained. After this, an overview will be given of possible ways to model the intracrial pressure system using white-box models. Finally, an analysis will be given of the usefulness of white-box models for ICP estimation.

5.1   The concept

A white-box model is a description of a system using information about its structure. The description results in a relationship between model input(for example arterial blood pressure) and output(for example intracranial pressure). A white-box model is composed using constitutive laws[21], interconnection laws[22] and parameters[23].

The model will always be a simplification of reality. This is necessary because reality is infinitely complex(even if we could model each molecule separately, we would still have to simplify). The trick is to make the right simplications in view of the purpose for which the model is designed. Because it is not always obvious what simplifications are right and also because the purpose of the models is not always the same, different models can exist for the same physical system[24].

White-box models can be used to estimate ICP in two ways. Firstly, by running the model using input from known sigals. The ICP value which results from this simulation can be used as an estimate for the real ICP. In this case, ICP is considered as a model variable. Secondly, the ICP could be considered as a

---

[19]Correlation after removing the effect of the other normalized harmonic intensity.

[20]Stepwise regression includes only the third harmonic

[21]A constitutive law describes the dynamic behavior of a system element. For example; the flow through a rigid tube is proportional to the pressure difference.

[22]An interconnection law describes the interconnection between elements. For example; when several blood vessels are connected at one point, the total incoming flows should be equal to the total outgoing flow.

[23]Numbers which determine the exact behavior of a constitutive law. For example; The normal parameter for a rigid tube is the resistance. Knowing the resistance and applying the constitutive law will result in the ability the calculate the flow from the pressure difference.

[24]A slightly unrealistic example; if you want to know how fast the coffee in a coffee mug will cool down, the model will focus on heat transfer and heat diffusion. If another researcher wants to throw the mug as far as possible, he will make an aerodynamic model of the mug. One physical reality, but two totally different models.

model parameter, influencing the behavior of the model. In this case parameter estimation of the model parameters using known signals should give an estimate for ICP.

In literature, only the first approach is used. The next section gives an overview of several model which were used to find ICP by simulation.

5.2   Possible models

Earlier research in this field [Hartman, 2011, Keizer, 2010] in UMC St. Radboud was mainly based on white-box models. Using anatomical knowledge of the human brain, a model was created to describe the relation between ABP, ICP and JVP. Extensive work has already been done in this field, mainly by Ursino[Ursino and Di Giammarco, 1991, Ursino and Lodi, 1997]. He included autoregulation in his model and did a lot of verification work on the model. Several others have proposed models, most of which are based on Ursino's model. The purpose of these models mainly is to increase understanding of phenomena in ICP dynamics[25]. Hu uses the white-box model developed by Ursino to estimate ICP or CBF[Hu et al., 2007]. Kashif does a similar thing, but with a lot of simplifications [Kashif et al., 2008].

Figures 10 and 11 gives an overview of the models introduced above. In the models, P denotes a pressure quantity, Q denotes a flow quantity, R denotes as resistance parameter and C denotes a compliance parameter. The notation is the same as in the mentioned papers and therefore, they can differ between models.

Keizer's model(figure 10(a)) consisted of the intracranial basin with five in- and outputs; Supply and drain of blood, formation and uptake of CSF and a fifth artificial connection which approximates the change in blood supply due to autoregulation(the autoregulation part was not defined in the report).

Hartman's model(figure 10(b)) proposal was more extensive. The blood flow is modeled as a flow through a resistor, CSF is generated from and reabsorbed in the blood and a compliance between the compartments is modeled. A distinction is also made between the brain matter and the ventricles. The model which was implemented(figure 10(c)), is less complex and resembles Keizer's model. Compared to that model, it lacks CSF drainage and autoregulation modeling.

The two implemented models have a substantial drawback. A lot of artificial processes are introduced (an extra input for modeling autoregulation, separate modeling of CSF formation), making it very hard to estimate or identify parameters. This makes the models hard to work with in practice. But also from a modeling point of view, it is a problem. Essentially, they are not a model of intracranial pressure dynamics, but a list of factors which can influence ICP.

Ursino made an extensive model for ICP modeling(figure 11(b)), visualized as an electronic network, which is common practice in this field). Later on, he devised a simplification of this model to limit the number of parameters and increase workability(figure 11(a)). The model consists of the following elements. At the point where arterial blood flow enters the brain, autoregulation takes place(modeled by a possible change in resistance and compliance of the smaller

---

[25]for example plateau waves

arteries). Via the capillaries(P_c) and the small veins(P_v), it flows to the venous system(P_{vs}). At the capillaries, CSF is generated from the blood stream, entering the intracranial compartment(P_{ic}). It is reabsorbed into the venous system. The intracranial compartment has some compliance(implemented as described by Marmarou[Marmarou et al., 1975]) and there is a possibility of CSF injection/drainage.

A big difference with the previous models is the fact that cerebral blood flow(CBF)[26] is considered an input in this model. In section 5.4, the advantage of this will be explained.

To be able to estimate ICP, Kashif[Kashif et al., 2008] further simplified Ursino's model, only keeping autoregulation and blood supply to the intracranial compartment. The estimation scheme can actually estimate ICP without calibration, using the arterial blood flow, but the parameter estimation is based on two assumptions. Firstly that during a sharp transition in ABP, the flow through the arteries is neglectable compared to the change in volume in the cerebral arteries. And secondly that ICP remains approximately constant within the heartbeat cycle. These assumptions seem plausible, but were not tested in the article.

Ursino's models have been through a great deal of validation and testing. Therefore, they can be considered valid for their purpose (modeling of intracranial pressure dynamics). For estimation purposes however, this is less clear. Hu concludes that his implementation does not work for ICP-estimation[Hu et al., 2007] and Kashif only tests using simulated data[Kashif et al., 2008].

5.3 Mathematical model properties

Keizer's model(figure 10(a)) is linear except for the autoregulation and the compliance of the cranium, which are not defined in the report. The compliance is the only dynamical part of the system. The rest of the model is static and the whole model is time-invariant.

Hartman's original model(figure 10(b)) is linear time-invariant and dynamic(because of the compliance). The model he used for simulation(figure 10(c)) is linear if the CSF pressure is considered an input. However, if it is considered as an internal time-varying parameter(as done in the report), the model becomes affine and time-variant.

Ursino's models(figure 11(b) and 11(a)) both contain a non-linear description of autoregulation and cranium compliance, making the systems non-linear. The systems are dynamic and time-invariant.

Non-linearity appears to be necessary to accurately model cerebral blood flow, because the auto-regulatory system influences the resistance and compliance of the arteries within the skull in a significant way. The system will also have to be dynamic to accurately model compliant behavior.

---

[26]The total blood flow into the brain.
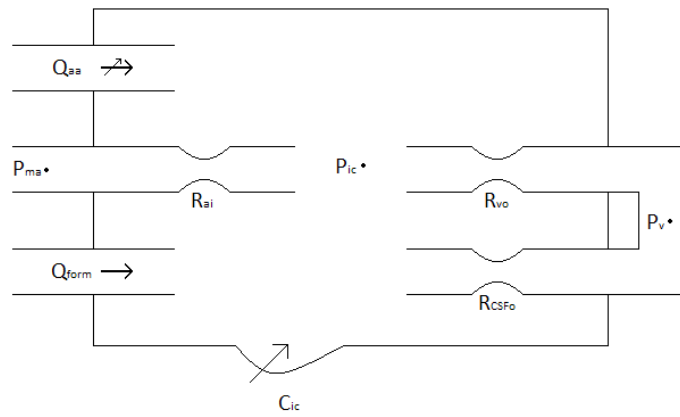
(a) Keizer's model (model constructed in [Keizer, 2010])
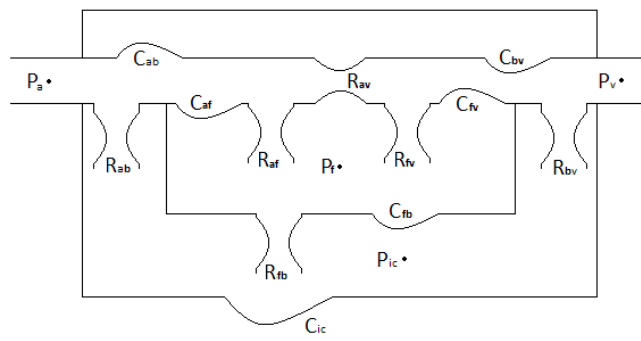
(b) Hartman's original model[Hartman, 2011]
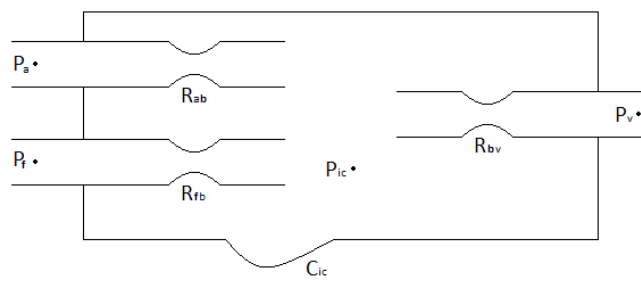
(c) Hartman's implemented model[Hartman, 2011]

Figure 10: model schematics

19
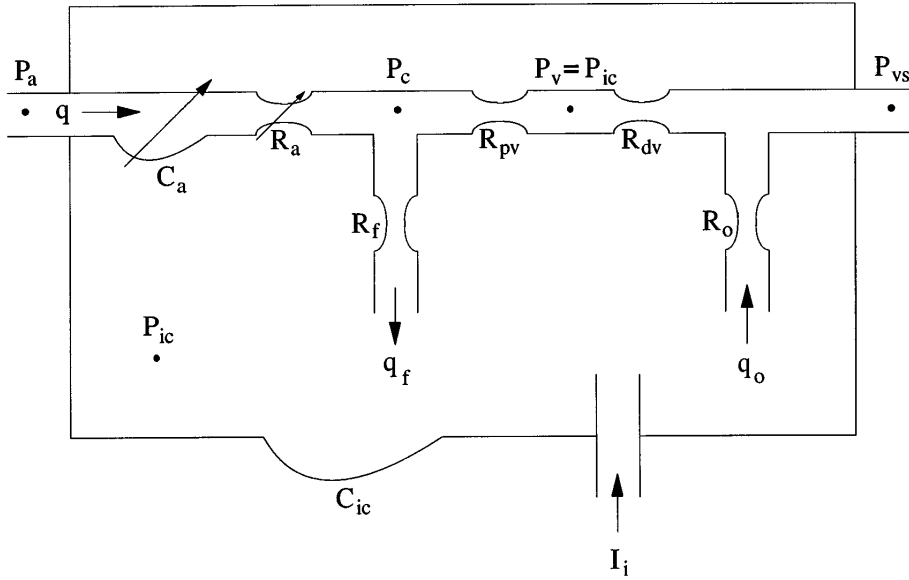
(a) model from Ursino and Lodi[Ursino and Lodi, 1997]
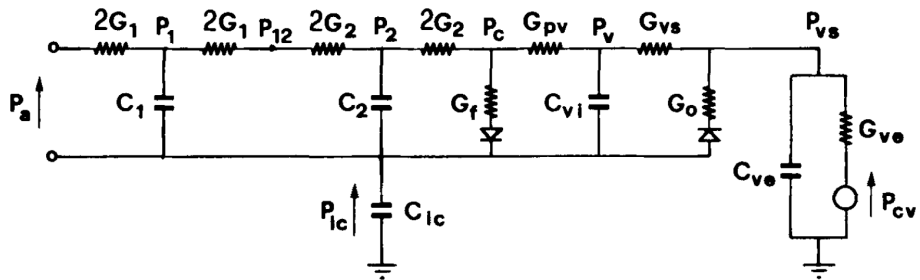
(b) electrical analogue of the extended model from Ursino[Ursino and Di Giammarco, 1991], some capacitances and resistors actually are variable
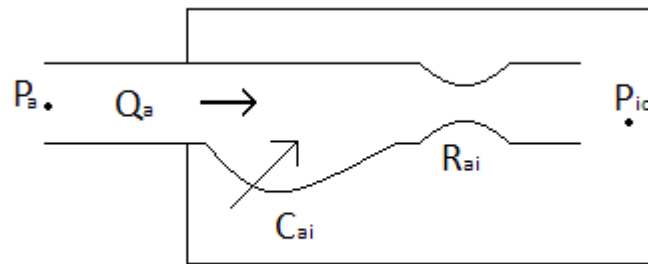
(c) Kashifs simplification of Ursino's model[Kashif et al., 2008]

Figure 11: Ursino model schematics and Kashifs simplification

5.4 Analysis of estimation by simulation

The first question is if estimation by simulation is possible when all input signals and parameters are perfectly known. First, the necessary elements for a model with this purpose are discussed and secondly, the input of such a model will be examined.

In the models, proposed in 5.2, cerebral autoregulation takes a prominent place. This can be easily justified, because this process is closely related to ICP. Omitting it in the model would make it a system which does not compensate for abnormal ICP values. Therefore, cerebral autoregulation should be included in the model. One could argue that this means that the model will inevitably become non-linear, because it contains elements with state-dependent parameters. On the other side, one could argue that when autoregulation operates within capacity, it behaves linear(flow is kept approximately constant). Including the possibility of failing autoregulation would result in a hybrid linear model[27], switching between constant flow(working autoregulation) and constant resistance/compliance(impaired autoregulation) in the arteries. Modeling autoregulation as either being intact or defective is based on the assumption that autoregulatory behavior is homogeneous, while this is often not the case.

Making an artificial distinction between normal flow and extra autoregulatory flow(as in Keizer's model) is not necessary. It does not add anything, but it only increases complexity.

Intracranial compliance is known to be non-linear[Marmarou et al., 1975] and because we are interested in relatively large ICP changes, linearization is not an option. This non-linear compliance behavior should therefore also be included. Specifying intracranial liquid flow(CSF generation and absorption) does not seem to be very necessary, because it all happens in the cranial compartment(so the ICP is not influenced). Moreover, because the veins collapse when the pressure drops below ICP(in figure 11(a), this is denoted as $P_v = P_{ic}$), the model will degenerate to a single intracranial compartment with one inflow and one outflow[28].

Possible input variables are arterial and venous blood pressure and cerebral blood flow(CBF).

If we have this model and enough input variables are known, it should be possible to give a good estimate of ICP. But even if this is possible, there are still some major problems, which might cause this approach to be infeasible.

Firstly, the problem of parameter estimation. Model parameters are generally not known and differ between patients. They can be found using an existing ICP-measurement data as done in [Hu et al., 2007]. This would mean that estimation can only been done after invasive measurement of the signal. And even then, estimation of autoregulatory function is difficult, because it is a complex phenomenon and it is often disturbed after acute brain injury.[29]. For an ac-

---

[27]A model which changes behavior when a certain value crosses a boundary. For example: if something falls into the sea, the behavior(fall acceleration) changes when it falls into the water.

[28]Anatomically, this distinction is still useful. CSF drainage obstruction is more intuitively modeled using the whole structure.

[29]In the past decades, a lot of research was dedicated to classify autoregulatory behavior using ICP measurements. This gives an indication of the challenge in estimating autoregulatory parameters

curate estimation of it's behavior, measurements from a broad ICP range are needed, which can usually not be obtained in a short calibration session.

Secondly, not all the inputs are easily measured. CBF can not be measured directly and therefore, it has to be estimated using flow velocity measurements. This gives an additional source of uncertainty. CBF is an important input variable, because it gives much information. Actually, it can be considered an output. When a certain arterial pressure is imposed on the system, CBF will give information about system properties, especially resistance.[30] Availability of accurate CBF measurements makes ICP estimation much more feasible.

And finally, a more fundamental problem arises when looking at the reasons for ICP monitoring. It is measured to be able to intervene when it increases above certain levels. Increased ICP is often caused by a change in the intracranial pressure system. For example; an infection in the ventricular system or internal hemorrhaging can partially block CSF drainage. This would mean that a model parameter(in this case the resistance to CSF drainage flow) changes. When using the model to estimate ICP, the model will fail to give a right estimate when this estimate is needed to detect a dangerous situation. This is illustrated by the fact that Hu's ICP estimation starts to deteriorate after a propofol injection. [Hu et al., 2007]

A similar argument holds for black-box models[31] Although it does not describe the structure in a direct way, it still tries to capture this structure and will therefore not be able to give right estimates by simulation when there is a change in structure which did not occur during calibration. Therefore, using a black-box model simulation to estimate ICP cannot accurately cope with new pathologies and therefore, it is of equally limited use in this case.

5.5 Changing model approach

As mentioned in the last section, modeling the brain for the purpose of ICP estimation is difficult, because many relevant factors in ICP change will be alterations of the model. It may be possible to use this. If we construct a model in which ICP influences the parameters, the estimated parameters of the model should give some information about ICP(figure 12 illustrates this idea). In our case, ABP and JVP can be used as input and output to estimate parameters a black-box ARX-model. Another approach would be to take the CVP into account as an input variable. If we find correlation between the mean ICP of the set and the model parameters we may be able to use this for ICP classification or estimation. A modeling downside to this method is that it was earlier observed that JVP is not only influenced along the bloodstream but also in the other direction. For this reason, a CVP-JVP blackbox model is also considered.

---

[30]Low resistance of will result in a high flow and vice versa.

[31]A black-box model is a model which describes the relation between in and outputs of a system without and a-priori assumption on system structure. It can be specified using measurements with known output
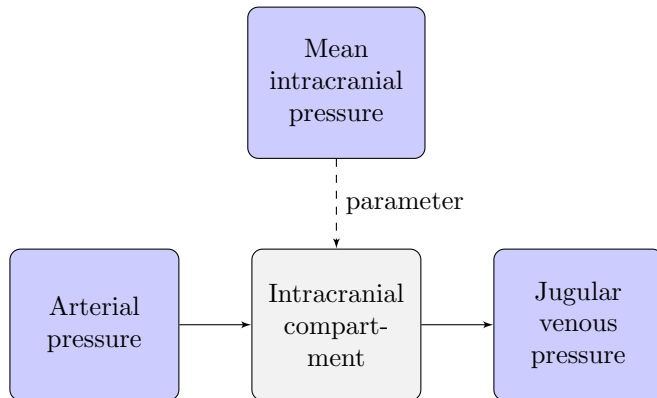
Figure 12: Mean intracranial pressure as a parameter in intracranial dynamics

5.5.1 The math

To model the JVP and the influence of ABP and CVP on this signal, we use an ARX-model:

$$
\begin{aligned}
y(k) + a_1 y(k-1) + \ldots + a_n y(k - n_a) = \\
b_0 u(k - n_k) + b_1 u(k - n_k - 1) + \ldots + b_{n_b - 1} u(k - n_k - n_b + 1) + e(k)
\end{aligned}
\tag{7}
$$

where $y(k)$ is the JVP signal, $u(k)$ the input signal(ABP or CVP), n_a and n_b are the model orders and n_k is the input delay. The input delay is calculated by calculating the mean distance between the heartbeat peak in the different signals.
Mathematical software(like MATLAB) can estimate the model parameters(a_i and b_i) using least-squares estimation techniques. This can be done for different samples. For each of these samples, we can also calculate the mean ICP. Using these mean ICP values, we can calculate $\rho_{x,ICP}$ and $p(\rho_{x,ICP} \neq 0)$ for $x \in a_1, \ldots, a_{n_a}, b_1, \ldots, b_{n_b}$.

5.5.2 Results

After mean subtracting, model coefficients were calculated for orders 1 to 6. The a-coefficients(describing the autoregressive part) were much bigger than the b-coefficients(input part). After compensating for the difference in signal amplitude[32], the difference between the contribution of the autoregressive part an the input part is in the order of magnitude of 10. This means that the model can be considered as an autonomous model with some external influence.
Tables 6 and 5 in appendix B.2 show the correlations between the model parameters for different model orders. The correlation is calculated for each patient and for the global set. The second number is the chance that the hypothesis

---

[32]the arterial pressure signal has an amplitude of around 70 mmHg, while the JVP has an amplitude of approximately 7 mmHg.

Hypothesis 5.1. *The correlation between the estimated parameter x_i of a kth order model and the mean ICP is zero.*

is true. Interpretation of this amount of p-values has to be done in a careful way. Small enough p-values will always arise when enough of them are calculated. Therefore, setting a threshold for significant correlation would not suffice in this case. Furthermore, the data is dominated by a relatively big set of measurements from one person, making it difficult to give any general statement.

Results from patient 1 and 2 do not give any indication for correlation between model parameters and mean ICP value. Without any extra information, low p-values for a_1 and b_1 at order 1, b_6 at order 6(patient 1) and b_5 at order 6(patient 2) can be considered coincidental. Results from patient 3 seem to be more structurally significant. a_1, a_2 and b_3(despite the low contribution of the input part to the model) have p-values below 0.05 for every order(except a_1 at order 3, which is slightly higher) and have the same sign. b_3 also shows relatively high correlations and sign consistency for patient 1 but not for patient 2(this could be due to the low amount of samples and low variation in ICP values). Results from model parameters when CVP is considered as an input(table 5) do no show any real significance in correlation. This is in accordance with results from section 3.

Because there are significant results from the autonomous part of the ARX-model[33], estimated parameter values for an AR-model(a black-box model without any input) for the JVP are also analyzed(table 7 in appendix B.2). The results for patient 3 are quite surprising. All correlations except one are significant. However, unlike the model with input, these results are not reflected in data from patients 1 and 2.
These are unexpected results. We were looking for the influence of the mean ICP value on the interconnection between ABP and JVP. In stead, the strongest result is the influence of ICP on the behavior/waveform of the JVP signal.

Based on the results, one could try to classify samples in the categories low ICP and high ICP, using one or two estimated model parameters. Figure 13(a) shows the values of the estimated parameter b_3 in a 5th order model for high(> 20 mmHg) and low(< 20 mmHg) ICP samples. This parameter was chosen because of good correlation values at different orders and consistency of correlation for patients 1 and 3. The boxplot shows that there is a clear distinction between the two categories($p = 0.025$). This is also true for the b_3 parameter for lower orders(p=0.015 for order 4 and p=0.025 for order 3), but it is less clear for order 6(p=0.111). This observation suggests that the ICP level influences the connection between the ABP and the JVP signal. However, it should again be noted that the samples are dominated by a large set of samples from one patient.
Figure 13(b) shows a scatter plot of the estimated a_1 parameter for a 3rd order AR-model and again the estimated b_3 parameter(from the 3rd order ARX-model) for one patient(patient 3). Because the low number of high ICP samples($n = 5$), an intermediate group($10 \leq ICP < 20$ mmHg) was formed

---

[33]The part which is not influenced by the input signal.

to get some more insight. The scatter plot shows a clear difference in distribution between the groups. The high ICP group and the intermediate group are located to the bottom left. The individual p-values for the two-sample t-test are not significant for high versus medium/low icp($p = 0.374$ for a_2 and b_3 for $p = 0.077$), but they are for high/medium versus low icp($p = 0.005$ for a_2 and b_3 for $p = 0.012$). However, these figure also make clear that ICP classification(into the classes high and normal ICP) based on these variables is not very accurate.
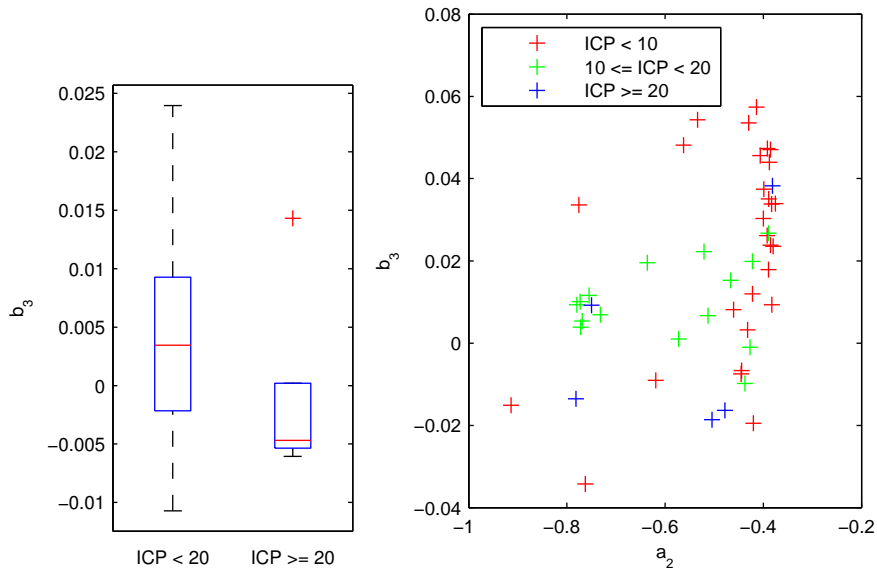
(a) estimated b_3 parameters in an order 5 ARX-model for low and high ICP measurements

(b) estimated a_2 and b_3 parameters in an order 3 ARX-model for low and high ICP measurements

Figure 13: Example of the possibility to distinguish high ICP based on estimated model parameters.

6 Detection of increased ICP

Based on results from previous sections, we can try to find a good measure for the detection of increased ICP($ICP > 20$ mmHg). To do this, stepwise regression[34] is applied to estimate the ICP value. This estimate is used to classify the measurement as indicating normal ICP or indicating increased ICP. As possible prediction values, we take the second and third harmonic relative intensities from the heartbeat waveform(see section 4). The values will be denoted as h_2 and h_3) and the 4th order model coefficients from section5.5 (denoted as a_1-a_4,b_1-b_4(arx-model) and aa_1-aa_4(ar-model)). The model coefficients for the CVP-JVP model are not included, because of their lack of correlation with ICP. Firstly, an analysis will be done of ICP level classification for patient 3, because of the available amount of data. Including only linear terms results in an estimation of ICP based on h_3, a_1 and b_3($R^2 = 0.60$). This is consistent with correlation results from 5.5. The estimation is shown in figure 14. The figure shows that estimation for patient 3 is rather good, but the regression coefficients cannot be used for the other patients($\rho = 0.21$ for the global set). The ROC-curve gives an overview of the possibility to use this estimate to detect increased ICP. In this dataset, increased ICP can be classified with a sensitivity[35] of 88% with a specificity[36] of 84%. The classifying power of the estimate is significant, but it has been used on the same dataset as the one used to do the regression analysis, so this result can only be considered indicative.

Adding non-linear terms to the regression analysis(such as h_3^2 or a_1b_3) only gives a marginal improvement($R^2 = 0.65$). Based on the scatter-plot, one could argue that the regression only seems to be working when the actual ICP is between 0 and 15 mmHg. This could indicate peacewise linear behavior[37].

Estimation of the global set gives the picture shown in figure 16(a)($R^2 = 0.35$, coefficients h_2,b_1 and b_3 are used). Again, the scatterplot(figures 16(a) and 16(b)) shows signs of peacewise linearity. The estimate seems to saturate between 10 and 20 mmHg. The distinction becomes even clearer when adding the square of the coefficients to the regression procedure(figure 16(b), b_4^2 aa_2^2 aa_4^2 are used as estimating variables, $R^2 = 0.44$). The break-point seems to be 12 mmHg. A ROC-curve of identification of slightly increased ICP($ICP > 12$ mmHg) is shown in figure 15. Stepwise regression analysis on the high ICP set(ICP> 12 mmHg) does not lead to any meaningful results($R^2 = 0.17$ in the linear case, $R^2 = 0.32$ when adding quadratic terms and cross products, which is very low for estimation with so many variables(119 in total)).

Including only samples with $ICP < 12$ mmHg, gives the scatterplot in figure 17(a)($R^2 = 0.49$ with parameters h_2 and a_2). A lot of improvement occurs when

---

[34]A procedure in which explaining variables are added or removed based on their explanatory value in the presence of the other included variables. The result is an estimation formula for ICP based on the previously included explaining variables.

[35]Percentage of the samples with $ICP > 20$ mmHg which are correctly identified as having increased ICP.

[36]Percentage of the samples with normal ICP which are correctly identified as having normal ICP. It's complement is the percentage of normal ICP samples which are wrongly defined as having increased ICP

[37]A system is peacewise linear is it if it has different behaviour for different ranges of a certain variable and for each range, the behavior is linear.

(a) ICP estimation using waveform an ARX-model parameters

(b) ROC-curve of identifying increased ICP($ICP > 20$ mmHg)
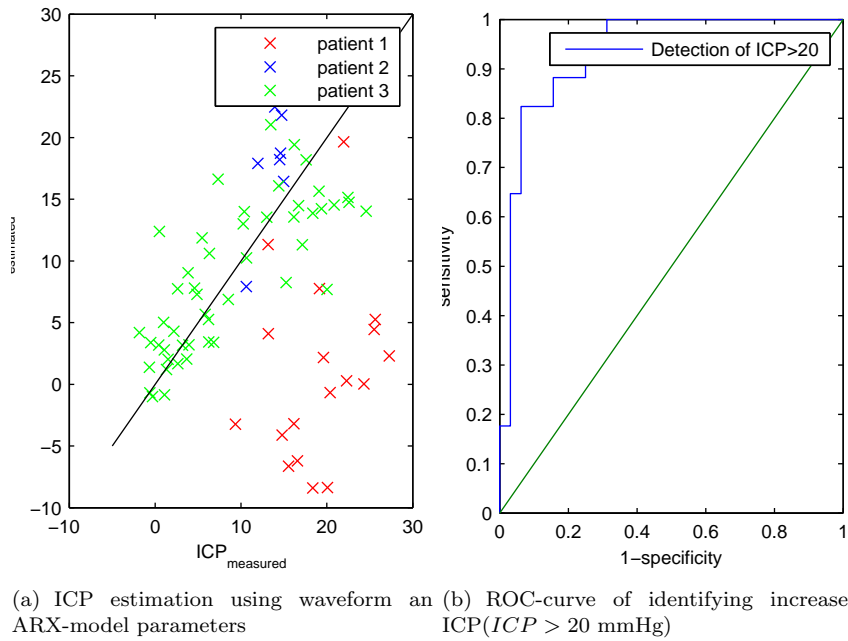
Figure 14: Patient-specific estimation and classification of ICP.
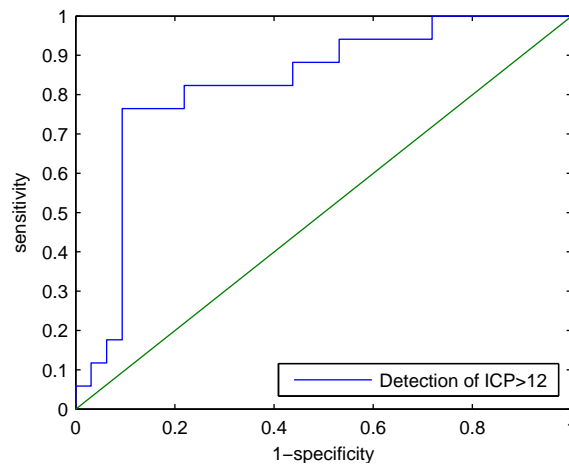
Figure 15: ROC-curve of identifying $ICP > 12$ mmHg

quadratic terms are added(figure 17(b)). h_2 and a_2 are still included, but the algorithm adds b_2, b_3 and aa_2. This could indicate non-linear behavior for low ICP(< 5 mmHg).

(a) ICP estimation using waveform and ARX-model parameters

(b) ICP estimation using waveform and ARX-model parameters, including their squares

Figure 16: Global(patient-aspecific) estimation of ICP

(a) ICP estimation using waveform and ARX-model parameters for ICP<12 mmHg

(b) ICP estimation using waveform and ARX-model parameters, including their squares for ICP<12 mmHg

Figure 17: Global(patient-aspecific) estimation of ICP for $ICP < 12$ mmHg.

7 Conclusion

Because of the low amount of data and the high number of different techniques which were exercised, all conclusions from this section are only preliminary. They can only be used to give directions for further research.

Based on anatomical knowledge, it seems obvious ABP will not be a very good indicator of ICP. It has an influence on the ICP, but will not be influenced by it. Based on this assumption, the ABP is not measured near the head, but in the arm, so based on the findings in this report, this assumption cannot be verified.
Correlation analysis did not show any interdependence between the JVP and the ICP signal(after correction for a mutual external source). The similarity between the ICP, JVP and CVP signal was studied. High similarity between CVP, JVP and ICP at high frequency(>0.3 Hz) was found. This indicates influence of ICP and JVP by CVP, because reverse influence would mean that a relatively small part of the venous system would dominate CVP dynamics. At low frequency(<0.3 Hz), the similarity between CVP and JVP weakens while the similarity between JVP and ICP stays the same. This indicates that there may be some ICP-influence on the JVP-signal at low frequency.

Using a model of the intracranial pressure system to estimate ICP has been tried before, but has some drawbacks which make it not very useful in clinical context. Due to parameter estimation, an estimation model will almost always have to be calibrated before use. And system changes due to pathologies could cause estimation errors when a good estimate is most important.

The influence of intracranial pressure could possibly influence the heartbeat waveform of the JVP signal. Second and third harmonic relative intensities of the JVP were calculated, and did correlate with mean ICP values. Another indication of ICP influence on the JVP is the correlation between ICP and estimated AR-model coefficients of the JVP-signal. However, the connection is very patient specific and not very strong. Therefore, on its own, it is not enough for reliable ICP estimation or increased ICP detection.

8 Discussion

We have seen that some information about ICP can be extracted from cerebral blood pressure signals, but reliable ICP estimation or classification is not possible.

One could wonder if there should not be more possibilities for ICP estimation using pressure signals. Physically, the lack of connection could be explained by the fact that ICP and JVP only have an indirect link. In figure 18, the way ICP influences JVP is shown in a schematic way. When pressure increases, it has an immediate influence on flow. Of course, other processes could influence this behavior(autoregulation plays an important role). Pressure in other compartments(for example JVP) is influenced by a change in flow over a certain

timespan[38]. This process can also be influenced by external factors(in our case high compliance of the veins and a relatively low resistance connection to the heart). It may well be possible that a weak connection is all that is left after these steps of influence.
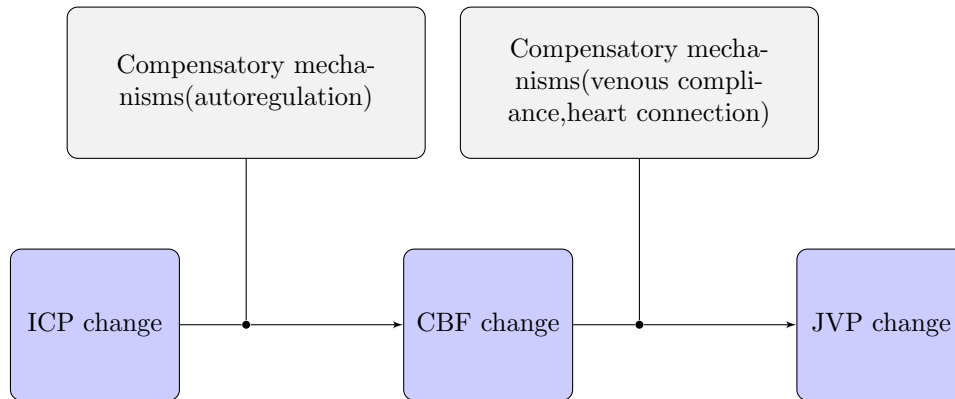
Figure 18: ICP influence on JVP

A lot of research in ICP estimation uses arterial flow velocity measurements measured by either doppler[Czosnyka et al., 1998, Aaslid et al., 1986, Belfort et al., 2000, Schmidt et al., 1997, Schmidt and Klingelhfer, 2002, Schmidt et al., 2003, Xu et al., 2010, Chacon et al., 2010] or MRI[Raksin et al., 2003, Alperin et al., 1996]. Some of this research shows promising results(for example [Chacon et al., 2010]). Estimating flow from flow velocity is still a challenge, but the usefulness of CBF estimates for ICP estimation is obvious; Flow into a certain compartment is directly influenced by the pressure within this compartment. Of course, because of mechanisms like cerebral autoregulation, this influence is not easily described. But still it can be expected to reveal more information about ICP than pressure signals.

Other approaches have also been introduced in literature. Some research has been done on the estimation of the ICP from IOP(intraocular pressure) and the behavior of the central retinal veins[Salman, 1997, Querfurth et al., 2004, Wu et al., 2009]. This results in a simple model, but it did not lead to any results yet. Czarnik[Czarnik et al., 2009] states that there is no significant correlation between IOP and ICP. Another possible approach is the use of MRI or other measurement devices to precisely measure the inner width of the skull. This distance should give some information about the pressure in the skull. This method is not suitable for continuous measurements and can therefore not be seen as a replacement for an intracranial probe.

The amount of possible parameters is a serious issue in this research. Study enough of them and some results will always surface. To counter this, extra attention was paid to consistency in results. Ideally, several decent sized sets of samples are used for this. Consistency in results for different sets indicates

---

[38]Pressure changes because volume is added to the compartment.

structural behavior. Because of the limited amount of available data, this could not be done to it's full extend.

The amount of data which was used to find estimators for ICP was limited. A lot of data was gathered from one patient(49 samples) with a lot of variation in ICP values. With this data, a decent analysis could be done for patient-specific ICP estimation. As mentioned earlier, the consistency of inner-patient results could not be checked fully because of this. Also, because of the low amount of samples from other patients(27 samples), general(not patient specific) ICP estimation could not be done properly. The reason for this is the dominance of the big set.
To properly analyze the methods proposed in this report, extensive measurement datasets(> 24 hours, preferable measured on several different days) should be acquired from multiple patients(≤ 4 for patient-specific ICP estimation, ≤ 10 for general ICP estimation). For general ICP estimation, shorter datasets could be used from more patients.

Estimation of ICP using waveform parameters resulted in an interesting observation. When the ICP is above 12 mmHg, the connection between ICP and JVP waveform parameters seems to disappear. A possible explanation for this is that the JVP waveform is influenced by the part of the time that the smaller veins collapse. Once ICP is above a certain threshold level(for example 12 mmHg), the part of the time in which the veins are open reaches a minimum to preserve blood flow.

In general, one could say that this research shed some light at the possibilities and problems of ICP estimation using pressure measurements. There certainly is a possibility of ICP estimation using pressure measurements, specifically using the heartbeat waveform of the JVP. But this estimate appears to be rather patient specific, so for each patient, calibration would be needed(for which ICP measurements are required). Also, the accuracy of the estimation is low, compared to the requirements for ICP measurement devices(error < 2 mmHg). Some methods using arterial blood flow velocity measurements, are much more accurate [Chacon et al., 2010, Xu et al., 2010]. It could be possible to use waveform parameters to refine the estimates of these methods.

References

[Aaslid et al., 1986] Aaslid, R., Lundar, T., Lindegaard, K.-F., and Nornes, H. (1986). Estimation of cerebral perfusion pressure from arterial blood pressure and transcranial Doppler recordings. In Miller, J., Teasdale, G., Rowan, J., Galbraith, S., and AD, M., editors, *Intracranial Pressure VI*, pages 226–9. Heidelberg: Springer-Verlag.

[Aaslid et al., 1982] Aaslid, R., Markwalder, T. M., and Nornes, H. (1982). Noninvasive transcranial Doppler ultrasound recording of flow velocity in basal cerebral arteries. *Journal of neurosurgery*, 57(6):769–774.

[Alperin et al., 1996] Alperin, N., Vikingstad, E. M., Gomez-Anson, B., and Levin, D. N. (1996). Hemodynamically independent analysis of cerebrospinal fluid and brain motion observed with dynamic phase contrast MRI. *Magnetic Resonance in Medicine*, 35(5):741–754.

[Belfort et al., 2000] Belfort, M. A., Tooke-Miller, C., Varner, M., Saade, G., Grunewald, C., Nisell, H., and Herd, J. A. (2000). Evaluation of a noninvasive transcranial Doppler and blood pressure-based method for the assessment of cerebral perfusion pressure in pregnant women. *Hypertension in Pregnancy*, 19(3):331–340.

[Chacon et al., 2010] Chacon, M., Pardo, C., Puppo, C., Curilem, M., and Landerretche, J. (2010). Non-invasive intracranial pressure estimation using support vector machine. In *Engineering in Medicine and Biology Society (EMBC), 2010 Annual International Conference of the IEEE*, pages 996 –999.

[Czarnik et al., 2009] Czarnik, T., Gawda, R., Kolodziej, W., Latka, D., Sznajd-Weron, K., and Weron, R. (2009). Associations between intracranial pressure, intraocular pressure and mean arterial pressure in patients with traumatic and non-traumatic brain injuries. *Injury*, 40(1):33 – 39.

[Czosnyka et al., 1998] Czosnyka, M., Matta, B. F., Smielewski, P., Kirkpatrick, P. J., and Pickard, J. D. (1998). Cerebral perfusion pressure in head-injured patients: a noninvasive assessment using transcranial Doppler ultrasonography. *Journal of Neurosurgery*, 88(5):802–808.

[Dugdale and Hoch, 2011] Dugdale, D. C. and Hoch, D. B. (2011). Intracranial pressure monitoring. `http://www.nlm.nih.gov/medlineplus/ency/imagepages/9480.htm`. Accessed on 05/07/2011.

[Hartman, 2011] Hartman, R. (2011). Determining ICP non-invasively: Is it possible? Final report about a Technical Medicine internship at the Radboud hospital, Nijmegen, University of Twente.

[Hellevik et al., 1999] Hellevik, L., Segers, P., Stergiopulos, N., Irgens, F., Verdonck, P., Thompson, C., Lo, K., Miyagishima, R., and Smiseth, O. (1999). Mechanism of pulmonary venous pressure and flow waves. *Heart and Vessels*, 14:67–71. 10.1007/BF02481745.

[Hu et al., 2007] Hu, X., Nenov, V., Bergsneider, M., Glenn, T., Vespa, P., and Martin, N. (2007). Estimation of hidden state variables of the intracranial

system using constrained nonlinear Kalman filters. *Biomedical Engineering, IEEE Transactions on*, 54(4):597 –610.

[INVOS, 2011] INVOS (2011). Explanation of the somanetics' INVOS system. `http://www.somanetics.com/our-technology/nirs-technology`. Accessed on 06/09/2011.

[Kashif et al., 2008] Kashif, F., Heldt, T., and Verghese, G. (2008). Model-based estimation of intracranial pressure and cerebrovascular autoregulation. In *Computers in Cardiology, 2008*, pages 369 –372.

[Keizer, 2010] Keizer, D. (2010). Measuring intracranial pressure. a physiological approach. Final report about a Technical Medicine internship at the Radboud hospital, Nijmegen, University of Twente.

[Koivistoinen et al., 2007] Koivistoinen, T., Kbi, T., Jula, A., Hutri-Khnen, N., Raitakari, O. T., Majahalme, S., Kukkonen-Harjula, K., Lehtimki, T., Reunanen, A., Viikari, J., and et al. (2007). Pulse wave velocity reference values in healthy adults aged 26-75 years. *Clinical Physiology and Functional Imaging*, 27(3):191–196.

[Kuwabara et al., 1992] Kuwabara, M., Nakajima, N., Yamamoto, F., Fujita, T., Takeuchi, S., Ando, M., Adachi, M., and Koga, Y. (1992). Continuous monitoring of blood oxygen saturation of internal jugular vein as a useful indicator for selective cerebral perfusion during aortic arch replacement. *J. Thorac. Cardiovasc. Surg.*, 103:355–362.

[Marmarou et al., 1975] Marmarou, A., Shulman, K., and LaMorgese, J. (1975). Compartmental analysis of compliance and outflow resistance of the cerebrospinal fluid system. *Journal of neurosurgery*, 43(5):523–534.

[Querfurth et al., 2004] Querfurth, H., Arms, S., Lichy, C., Irwin, W., and Steiner, T. (2004). Prediction of intracranial pressure from noninvasive transocular venous and arterial hemodynamic measurements. *Neurocritical Care*, 1:183–194. 10.1385/NCC:1:2:183.

[Raksin et al., 2003] Raksin, P. B., Alperin, N., Sivaramakrishnan, A., Surapaneni, S., and Lichtor, T. (2003). Noninvasive intracranial compliance and pressure based on dynamic magnetic resonance imaging of blood flow and cerebrospinal fluid flow: review of principles, implementation, and other noninvasive approaches. *Neurosurgical focus [electronic resource].*, 14(4).

[Rebuck et al., 2000] Rebuck, J. A., Murry, K. R., Rhoney, D. H., Michael, D. B., and Coplin, W. M. (2000). Infection related to intracranial pressure monitors in adults: analysis of risk factors and antibiotic prophylaxis. *Journal of Neurology, Neurosurgery & Psychiatry*, 69(3):381–384.

[Salman, 1997] Salman, M. S. (1997). Can intracranial pressure be measured non-invasively? *Lancet*, 350(9088):1367.

[Schmidt et al., 2003] Schmidt, B., Czosnyka, M., Raabe, A., Yahya, H., Schwarze, J. J., Sackerer, D., Sander, D., and Klingelhofer, J. (2003). Adaptive noninvasive assessment of intracranial pressure and cerebral autoregulation. *Stroke*, 34(1):84–89.

[Schmidt and Klingelhfer, 2002] Schmidt, B. and Klingelhfer, J. (2002). Clinical applications of a non-invasive icp monitoring method. *European Journal of Ultrasound*, 16(1-2):37 – 45.

[Schmidt et al., 1997] Schmidt, B., Klingelhofer, J., MD, J., Schwarze, J. J., Sander, D., and Wittich, I. (1997). Noninvasive prediction of intracranial pressure curves using transcranial Doppler ultrasonography and blood pressure curves. *Stroke*, 28(12):2465–2472.

[Smielewski et al., 1997] Smielewski, M., Kirkpatrick, P., Laing, P., Menon, R., Pickard, D., and Czosnyka, J. (1997). Continuous assessment of the cerebral vasomotor reactivity in head injury. *Neurosurgery*, 41(1):11–19.

[Ursino and Di Giammarco, 1991] Ursino, M. and Di Giammarco, P. (1991). A mathematical model of the relationship between cerebral blood volume and intracranial pressure changes: The generation of plateau waves. *Annals of Biomedical Engineering*, 19(1):15–42.

[Ursino and Lodi, 1997] Ursino, M. and Lodi, C. A. (1997). A simple mathematical model of the interaction between intracranial pressure and cerebral hemodynamics. *Journal of applied physiology*, 82(4):1256–1269.

[Wu et al., 2009] Wu, S., Xu, P., Asgari, S., Bergsneider, M., and Hu, X. (2009). Time series mining approach for noninvasive intracranial pressure assessment: An investigation of different regularization techniques. In *Computer Science and Information Engineering, 2009 WRI World Congress on*, volume 5, pages 382 –386.

[Xu et al., 2010] Xu, P., Kasprowicz, M., Bergsneider, M., and Hu, X. (2010). Improved noninvasive intracranial pressure assessment with nonlinear kernel regression. *Information Technology in Biomedicine, IEEE Transactions on*, 14(4):971 –978.

A   Datasets and samples

In table 2, the datasets which were used in this report are described. In table 3, the 10-minute samples which were used for analysis are shown.

Name	Patient Code	Date	Start time	End time	Remarks
DatasetA1	2	01-12-2010	14.49u	15.53u	
DatasetA2	2	02-12-2010	11.00u	13.00u	
DatasetB1	1	20-12-2010	12.30u	15.30u	
DatasetB2	1	21-12-2010	9.30u	15.00u	
DatasetB3	1	22-12-2010	9.15u	15.30u	
DatasetB4	1	23-12-2010	8.30u	11.30u	
DatasetC1	3	04-04-2011	15.35u	16.10u	CVP also recorded
DatasetC2	3	04/05-04-2011	16.15u	0.15u	CVP also recorded
DatasetC3	3	05-04-2011	0.15u	7.50u	CVP also recorded
DatasetC4	3	08-04-2011	14.53u	17.36u	CVP also recorded

Table 2: Dataset information.

Sample number	Dataset	Start time(sec)	Mean ICP	Mean heartbeat frequency(Hz)	Mean breath frequency(Hz)	PRx
1	datasetB1	2000	13.2	1.10	0.40	-0.04
2	datasetB1	7600	20.4	1.04	0.45	-0.09
3	datasetB2	4000	15.5	1.09	0.42	-0.23
4	datasetB2	11600	16.2	1.03	0.42	-0.21
5	datasetB2	19400	13.2	1.09	0.42	-0.29
6	datasetB3	100	27.3	1.18	0.42	0.01
7	datasetB3	3800	25.6	1.15	0.42	-0.19
8	datasetB3	7400	19.6	1.22	0.47	-0.12
9	datasetB3	11000	22.3	1.17	0.47	-0.35
10	datasetB3	13300	24.3	1.11	0.47	-0.28
11	datasetB3	16800	9.3	1.16	0.47	-0.48
12	datasetB4	350	19.1	1.20	0.47	-0.49
13	datasetB4	1100	25.5	1.20	0.47	0.00
14	datasetB4	2050	21.9	1.16	0.47	-0.04
15	datasetB4	4200	14.8	1.08	0.47	-0.21
16	datasetB4	6700	16.6	1.14	0.47	-0.34
17	datasetB4	8000	18.4	1.10	0.47	-0.04
18	datasetB4	9800	20.1	1.10	0.47	-0.30
19	datasetA1	200	12.0	1.03	0.27	0.17
20	datasetA1	1900	11.2	0.94	0.27	0.12
21	datasetA1	3200	10.6	0.97	0.27	0.13
22	datasetA2	2460	14.5	0.98	0.27	-0.11
23	datasetA2	3060	14.6	0.98	0.27	0.34
24	datasetA2	3660	13.9	0.95	0.27	-0.06
25	datasetA2	5300	14.8	0.92	0.27	0.31
26	datasetA2	5900	15.0	0.94	0.27	0.13
27	datasetA2	7700	20.9	1.00	0.27	0.30
28	datasetC1	970	7.3	1.19	0.25	0.09
29	datasetC2	1500	22.6	1.23	0.25	0.70
30	datasetC2	2100	22.4	1.23	0.25	0.35
31	datasetC2	3400	10.3	1.21	0.25	0.25
32	datasetC2	4200	10.6	1.21	0.25	0.12
33	datasetC2	5400	6.3	1.21	0.25	0.22
34	datasetC2	8600	13.5	1.17	0.25	0.08
35	datasetC2	9600	16.2	1.15	0.25	0.17
36	datasetC2	10800	15.2	1.17	0.25	0.15
37	datasetC2	11900	16.2	1.14	0.25	0.13
38	datasetC2	14500	17.2	1.12	0.25	0.15
39	datasetC2	15700	24.6	1.08	0.25	0.21
40	datasetC2	16800	16.7	1.14	0.25	0.39
41	datasetC2	17600	19.1	1.13	0.25	0.16
42	datasetC2	18300	18.4	1.13	0.25	0.30
43	datasetC2	19000	19.4	1.13	0.25	0.17
44	datasetC2	19700	20.9	1.14	0.25	0.33
45	datasetC2	21600	4.9	1.28	0.25	0.06
46	datasetC2	22200	5.8	1.29	0.25	0.20
47	datasetC2	22850	5.5	1.30	0.25	-0.16
48	datasetC2	24400	14.4	1.21	0.25	0.30
49	datasetC2	25300	10.4	1.21	0.25	-0.26
50	datasetC2	26200	13.0	1.20	0.25	0.26
51	datasetC2	27900	17.6	1.14	0.25	0.35
52	datasetC3	300	20.0	1.24	0.25	0.39
53	datasetC3	2500	1.0	1.38	0.25	0.49
54	datasetC3	3150	0.4	1.36	0.25	0.58
55	datasetC3	3800	-0.7	1.36	0.25	0.55
56	datasetC3	4450	-0.6	1.33	0.25	0.58
57	datasetC3	5400	-1.8	1.29	0.25	0.49
58	datasetC3	7500	-0.5	1.22	0.25	0.42
59	datasetC3	10500	1.5	1.13	0.25	0.28
60	datasetC3	11200	2.7	1.15	0.25	0.29
61	datasetC3	12000	3.2	1.13	0.25	0.36
62	datasetC3	12900	4.6	1.12	0.25	0.22
63	datasetC3	16600	6.8	1.12	0.25	0.21
64	datasetC3	17350	6.3	1.11	0.25	0.17
65	datasetC3	18500	6.2	1.12	0.25	0.34
66	datasetC3	19900	8.5	1.17	0.25	0.21
67	datasetC3	21000	3.8	1.18	0.25	0.13
68	datasetC3	23900	3.7	1.17	0.25	0.31
69	datasetC3	24600	2.2	1.15	0.25	0.30
70	datasetC4	800	-0.3	0.98	0.28	-0.05
71	datasetC4	2100	1.3	0.97	0.28	-0.01
72	datasetC4	4600	3.9	0.94	0.28	0.22
73	datasetC4	6400	1.1	1.01	0.28	-0.07
74	datasetC4	7000	0.5	0.98	0.28	-0.11
75	datasetC4	8200	1.1	0.89	0.28	-0.27
76	datasetC4	9000	2.6	0.87	0.28	0.11

Table 3: 10-minute samples information. Start times are relative to the start of the dataset

B   Tables and figures

B.1   Higher harmonics correlations

	Respiratory wave		Heartbeat wave	
	2nd harmonic	3rd harmonic	2nd harmonic	3rd harmonic
patient 1($n = 18$)	0.01 (0.960)	0.25 (0.325)	0.55 (0.019)	0.59 (0.009)
patient 2($n = 9$)	0.37 (0.009)	0.77 (0.014)	-0.42 (0.263)	0.14 (0.712)
patient 3($n = 49$)	0.16 (0.259)	-0.17 (0.232)	0.52 (0.000)	0.61 (0.000)
global($n = 76$)	0.11	0.10	0.44	0.32

Table 4: Correlation coefficients between normalized 2nd and 3rd harmonic intensities and mean ICP values with $P(\rho = 0)$(the chance that there is no correlation). p-values for the total set are not given, because the samples are not independent.

B.2   ARX-model parameter correlations

	a_1	a_2	a_3	a_4	a_5	a_6	b_1	b_2	b_3	b_4	b_5	b_6
						Patient 3($n = 49$)						
1	-0.36 (0.013)						0.15 (0.311)					
2	-0.16 (0.265)	0.15 (0.293)					0.38 (0.009)	-0.26 (0.082)				
3	-0.16 (0.276)	-0.15 (0.336)	0.16 (0.275)				0.33 (0.022)	0.06 (0.701)	-0.23 (0.118)			
4	-0.21 (0.150)	-0.25 (0.082)	0.27 (0.065)	0.24 (0.091)			0.17 (0.246)	0.15 (0.305)	0.13 (0.384)	-0.24 (0.098)		
5	-0.31 (0.030)	-0.28 (0.054)	0.15 (0.364)	0.20 (0.170)	0.29 (0.040)		-0.04 (0.802)	0.08 (0.577)	0.27 (0.061)	-0.01 (0.941)	0.00 (0.990)	
6	-0.29 (0.042)	-0.28 (0.052)	-0.02 (0.900)	0.21 (0.148)	0.24 (0.094)	0.14 (0.358)	-0.12 (0.437)	0.01 (0.927)	0.17 (0.261)	-0.07 (0.626)	-0.03 (0.838)	0.26 (0.083)

Table 5: Correlation coefficients between estimated ARX model parameters with CVP input and mean ICP values with $P(\rho = 0)$(the chance that there is no correlation). p-values for the total set are not given, because the samples are not independent.

	a_1	a_2	a_3	a_4	a_5	a_6	b_1	b_2	b_3	b_4	b_5	b_6
Patient 1($n = 18$)												
1	0.82 (0.000)						-0.58 (0.011)					
2	-0.24 (0.339)	0.25 (0.312)					-0.32 (0.214)	0.29 (0.250)				
3	0.11 (0.673)	-0.12 (0.635)	0.14 (0.596)				-0.27 (0.272)	0.24 (0.334)	0.18 (0.481)			
4	-0.17 (0.541)	-0.31 (0.220)	0.22 (0.379)	-0.25 (0.309)			-0.12 (0.649)	0.26 (0.325)	-0.29 (0.247)	0.36 (0.142)		
5	0.04 (0.889)	-0.43 (0.085)	0.18 (0.473)	0.05 (0.846)	-0.04 (0.889)		-0.08 (0.746)	0.22 (0.408)	-0.42 (0.087)	0.23 (0.362)	0.40 (0.104)	
6	0.31 (0.226)	-0.52 (0.033)	0.20 (0.425)	0.08 (0.763)	-0.03 (0.895)	-0.14 (0.582)	-0.04 (0.866)	0.35 (0.179)	-0.36 (0.142)	0.29 (0.251)	0.34 (0.171)	0.36 (0.184)
Patient 2($n = 9$)												
1	-0.14 (0.723)						0.20 (0.662)					
2	0.31 (0.454)	-0.37 (0.361)					0.03 (0.931)	-0.01 (0.981)				
3	0.23 (0.581)	-0.23 (0.583)	0.23 (0.592)				-0.33 (0.383)	-0.08 (0.837)	0.39 (0.304)			
4	-0.10 (0.834)	-0.01 (0.978)	0.03 (0.942)	0.24 (0.539)			-0.38 (0.311)	-0.40 (0.292)	0.12 (0.765)	0.57 (0.110)		
5	0.11 (0.795)	0.07 (0.877)	-0.07 (0.848)	0.53 (0.138)	-0.49 (0.219)		0.12 (0.768)	-0.28 (0.460)	-0.03 (0.936)	0.61 (0.081)	-0.56 (0.115)	
6	0.48 (0.189)	-0.16 (0.699)	-0.05 (0.903)	0.48 (0.189)	0.04 (0.916)	-0.41 (0.267)	-0.22 (0.596)	-0.20 (0.611)	-0.06 (0.887)	0.64 (0.061)	-0.82 (0.007)	-0.11 (0.778)
Patient 3($n = 49$)												
1	-0.41 (0.003)						0.10 (0.491)					
2	-0.67 (0.000)	0.54 (0.000)					-0.45 (0.001)	-0.39 (0.005)				
3	-0.27 (0.075)	0.31 (0.042)	-0.30 (0.045)				-0.26 (0.077)	-0.34 (0.017)	-0.34 (0.018)			
4	-0.38 (0.010)	0.30 (0.037)	-0.22 (0.144)	0.06 (0.689)			-0.21 (0.163)	-0.16 (0.285)	-0.31 (0.030)	-0.06 (0.706)		
5	-0.59 (0.000)	0.35 (0.018)	-0.05 (0.726)	-0.19 (0.185)	0.21 (0.147)		-0.15 (0.312)	-0.13 (0.371)	-0.37 (0.010)	-0.08 (0.567)	0.09 (0.527)	
6	-0.57 (0.000)	0.36 (0.014)	0.01 (0.958)	-0.13 (0.374)	-0.03 (0.836)	0.12 (0.401)	-0.26 (0.077)	-0.11 (0.456)	-0.38 (0.007)	-0.09 (0.552)	-0.03 (0.822)	0.25 (0.088)
Global($n = 76$)												
1	-0.50						-0.13					
2	0.03	-0.13					-0.54	-0.49				
3	0.26	-0.26	0.27				-0.42	-0.43	-0.44			
4	0.23	-0.18	-0.17	0.30			-0.36	-0.26	-0.44	-0.07		
5	0.16	-0.16	-0.11	0.04	0.09		-0.20	-0.21	-0.43	-0.16	-0.03	
6	0.15	-0.15	-0.11	0.06	0.02	-0.02	-0.30	-0.14	-0.41	-0.12	-0.09	0.12

Table 6: Correlation coefficients between estimated ARX model parameters with CVP input and mean ICP values with the $P(\rho = 0)$(the chance that there is no correlation). p-values for the total set are not given, because the samples are not independent.

	a_1	a_2	a_3	a_4	a_5	a_6
Patient 1$(n = 18)$						
1	-0.83 (0.000)					
2	-0.07 (0.783)	0.03 (0.915)				
3	-0.08 (0.760)	-0.04 (0.885)	0.07 (0.781)			
4	-0.10 (0.702)	-0.56 (0.020)	0.02 (0.923)	0.18 (0.463)		
5	-0.10 (0.701)	-0.52 (0.032)	-0.06 (0.828)	0.05 (0.848)	0.38 (0.117)	
6	-0.06 (0.816)	-0.32 (0.199)	-0.09 (0.715)	-0.05 (0.838)	0.15 (0.553)	0.22 (0.377)
Patient 2$(n = 9)$						
1	0.28 (0.504)					
2	0.07 (0.867)	-0.05 (0.897)				
3	0.14 (0.741)	0.15 (0.716)	-0.23 (0.587)			
4	0.14 (0.734)	0.19 (0.648)	-0.35 (0.390)	-0.08 (0.828)		
5	0.13 (0.760)	0.16 (0.701)	-0.30 (0.465)	-0.40 (0.330)	0.07 (0.874)	
6	0.19 (0.648)	0.13 (0.767)	-0.32 (0.433)	-0.74 (0.034)	-0.30 (0.438)	0.34 (0.403)
Patient 3$(n = 49)$						
1	-0.50 (0.000)					
2	-0.51 (0.000)	0.52 (0.000)				
3	-0.53 (0.000)	-0.26 (0.082)	0.54 (0.000)			
4	-0.46 (0.001)	-0.55 (0.000)	0.40 (0.004)	0.50 (0.000)		
5	-0.46 (0.001)	-0.57 (0.000)	0.50 (0.000)	0.47 (0.001)	0.56 (0.000)	
6	-0.43 (0.002)	-0.58 (0.000)	-0.60 (0.000)	0.43 (0.002)	0.51 (0.000)	0.60 (0.000)
Global$(n = 76)$						
1	-0.25					
2	-0.45	0.46				
3	-0.41	-0.33	0.43			
4	-0.47	-0.48	0.43	0.49		
5	-0.50	-0.53	0.04	0.50	0.49	
6	-0.49	-0.56	-0.44	0.42	0.53	0.42

Table 7: Correlation coefficients between estimated ARX model parameters with CVP input and mean ICP values with $P(\rho = 0)$(the chance that there is no correlation). p-values for the total set are not given, because the samples are not independent.